Dalton Transactions

ROYAL SOCIETY OF CHEMISTRY

PAPER

View Article Online
View Journal | View Issue

Check for updates

Cite this: *Dalton Trans.*, 2026, **55**, 3111

Open Access Article. Published on 29 January 2026. Downloaded on 6/15/2026 11:04:01 PM.
This article is licensed under a Creative Commons Attribution-NonCommercial 3.0 Unported Licence.

Efficient *in situ* reduction and recovery of neptunium(V) using redox-functionalized deep eutectic solvents

Lin Zhang,† Qilong Tang,† Zhipeng Wang * and Chao Xu *

Received 29th December 2025,
Accepted 28th January 2026

DOI: 10.1039/d5dt03100a

rsc.li/dalton

The separation and recovery of neptunium (Np) represents a critical challenge in nuclear waste reprocessing. To address the difficulty of effectively capturing Np(V) in conventional extraction systems, this study designed and constructed three hydrophobic deep eutectic solvents (DESs) using tri-*n*-octylphosphine oxide (TOPO) as the hydrogen bond acceptor (HBA) and dihydroxybenzene isomers (catechol, CC; resorcinol, RC; hydroquinone, HQ) as hydrogen bond donors (HBD). These DESs enabled the *in situ* reduction at the liquid–liquid interface and highly efficient extraction of Np(V). Among them, the TOPO-CC DES system exhibited outstanding extraction performance for Np(V) over a broad acidity range of 10^{-3} to 2.0 M HNO_3, achieving a single-stage distribution ratio (D_{Np}) up to 85 and an *in situ* reduction conversion ratio from Np(V) to Np(IV) exceeding 98% within 5 minutes. Mechanistic investigations revealed that the extraction process follows a "coordination-driven reduction" mechanism. TOPO initially forms a weak coordination intermediate with Np(V) at the interface, thereby lowering its reduction potential. Subsequently, the dihydroxybenzene component facilitates efficient electron transfer within the organic phase, reducing Np(V) to Np(IV), which is strongly complexed and extracted by TOPO, completing an integrated "coordination–reduction–extraction" process. Furthermore, this system maintained stable extraction performance under challenging conditions, including high salinity (1–5 M $NaNO_3$), a wide temperature range (293–313 K), and significant cumulative γ irradiation doses (up to 60 kGy). This study provides a novel integrated DES strategy for the efficient and green recovery of Np(V) and lays a scientific foundation for the application of functionalized deep eutectic solvents in advanced nuclear fuel cycles.

Introduction

The sustainable development of nuclear energy is a crucial strategy for ensuring future energy security and addressing climate change. One of its core challenges lies in the safe, efficient management, and resource recovery of high-level radioactive waste. In spent nuclear fuel reprocessing, the separation and recovery of actinide elements are particularly important, as they are directly related to the volume reduction and hazard control of radioactive waste, as well as the economic viability and sustainability of the nuclear fuel cycle.[1–4] Among the various actinides, neptunium (Np) stands out as a key difficulty and limiting factor in separation process design and optimization due to its complex redox behavior and unique chemical properties.[5] In typical reprocessing systems employing nitric acid media, Np commonly exists in three oxidation states (Np(IV), Np(V), and Np(VI)) in dynamic equilibrium, with their distribution influenced by multiple factors such as solution acidity, ionic strength, radiation field, and coexisting ions.[6–8] Notably, pentavalent neptunium (Np(V)) exists as the linear NpO_2^+ cation. The low effective charge on the central Np atom (approximately +2.2) and the stability of its hydration shell result in very weak coordination between this species and most conventional extractants (*e.g.*, neutral organophosphorus compounds, amides, *etc.*), leading to low extraction efficiency and difficulty in achieving effective separation and enrichment in traditional solvent extraction systems.[9,10] This characteristic causes Np(V) to be prone to loss or improper distribution during reprocessing flowsheets, not only increasing the long-term environmental risk of high-level waste but also potentially affecting the purity of key nuclear product streams, such as plutonium (Pu) and uranium (U). Therefore, achieving the efficient and selective recovery of Np, especially the chemically inert Np(V), represents a significant scientific and technological challenge in the field of nuclear fuel cycles.[11–17]

One widely recognized effective strategy involves reduction conversion, transforming the poorly extractable Np(V) into the readily extractable tetravalent Np(IV), whose extraction behavior is similar to that of Pu(IV) and can be effectively captured using

---

Institute of Nuclear and New Energy Technology, Tsinghua University, 100084 Beijing, China. E-mail: wangzhipeng@mail.tsinghua.edu.cn

† These authors contributed equally to this work.

Open Access Article. Published on 29 January 2026. Downloaded on 6/15/2026 11:04:01 PM.
This article is licensed under a Creative Commons Attribution-NonCommercial 3.0 Unported Licence.

existing extraction systems.[5,18] However, the reduction process from Np(v) to Np(iv) involves oxygen atom removal and simultaneous electron transfer, characterized by slow kinetics and high thermodynamic barriers and high thermodynamic barriersed,[18–21] as evidenced by relevant electrochemical studies.[22,23] While such chemical reductants can promote reduction to some extent, their application faces notable limitations. Reduction efficiency is highly dependent on medium conditions, potentially generating secondary polluting by-products. Moreover, their introduction often interferes with the chemical states and extraction equilibria of other actinides or fission products in the system, increasing the complexity of process control.[24] Consequently, developing a novel functionalized system capable of synchronously achieving the reduction and subsequent extraction of Np(v) within the same medium without introducing external reagents is regarded as a crucial research direction to overcome current technological bottlenecks, holding both fundamental theoretical value and practical application potential.

In recent years, deep eutectic solvents (DESs) have attracted widespread attention as a class of green solvent systems formed through hydrogen bonding and other intermolecular interactions between a hydrogen bond acceptor (HBA) and a hydrogen bond donor (HBD).[25–27] Compared to traditional molecular solvents and ionic liquids, DESs offer numerous advantages, such as low vapor pressure, low toxicity, good biocompatibility, simple preparation, relatively low cost, and the ability to systematically tune their physicochemical properties (*e.g.*, viscosity, polarity, solubility) by flexibly selecting or designing HBA and HBD components.[28–31] Furthermore, the design and construction of DESs enables direct liquefaction of the extractant. The resulting deep eutectic solvent contains an extremely high concentration of the extractant, eliminating the need for additional diluents.[32] For instance, Gilmore *et al.*[28] designed and constructed a deep eutectic solvent formed by TOPO/phenol, which demonstrated excellent extraction performance for UO_2^{2+} in acidic solutions. Hao *et al.*[30] investigated the role and mechanisms of three DGA/phenol DESs in the separation of radionuclides such as U, Np, Pu, and Am. More importantly, the structural tunability of DESs provides a unique platform for constructing multifunctional solvents that combine metal ion coordination capability with redox activity. By rationally selecting component molecules with specific functions, DESs can simultaneously act as both a reducing medium and an extraction phase during separation processes, enabling the integration of metal ion oxidation state control and extraction separation.

Based on this background, this study aims to design and construct a novel class of hydrophobic functionalized DESs for the efficient and green recovery of Np(v) from nitric acid media. The study selects the neutral organophosphorus extractant tri-*n*-octylphosphine oxide (TOPO), known for its strong coordination ability and high selectivity for tetravalent actinide ions, as the HBA.[33] Concurrently, to endow the system with reducing functionality, a series of dihydroxybenzene compounds with *ortho*-, *meta*-, and *para*-isomeric structures, namely catechol (CC), resorcinol (RC), and hydroquinone (HQ), are chosen as HBDs. Through molecular self-assembly, three corresponding hydrophobic DESs were successfully prepared: TOPO-CC DES, TOPO-RC DES, and TOPO-HQ DES. This study systematically investigated the extraction behavior of these three functionalized DESs towards Np(v) in the aqueous phase, detailing the effects of conditions such as acidity, contact time, and temperature on extraction efficiency. Furthermore, analytical techniques including absorption spectroscopy and nuclear magnetic resonance were employed to characterize the species distribution, valence state changes, and possible coordination forms in the organic and aqueous phases before and after extraction. The goal is to elucidate the coupled reduction–extraction mechanism of Np(v) in the DES medium, reveal the influence of HBD structural differences on reducing capability and extraction performance, and thereby provide theoretical basis and technical reference for developing novel integrated actinide separation systems.

Experimental section

Chemicals and materials

TOPO (purity > 98%) was purchased from Shanghai Aladdin Biochemical Technology Co., Ltd. Catechol, resorcinol, hydroquinone, and *n*-dodecane, all of analytical grade, were obtained from Sinopharm Chemical Reagent Co., Ltd. Inorganic reagents such as nitric acid (HNO_3) and sodium nitrate ($NaNO_3$) were of guaranteed reagent grade. Ultrapure water (resistivity $\geq$ 18.2 MΩ cm) was used throughout the experiments. The Np-237 tracer solution was provided by the Institute of Nuclear and New Energy Technology at Tsinghua University.

Caution: Np-237 is an alpha-emitting radionuclide. All operations were conducted in dedicated radiochemical laboratories in strict compliance with radiation protection protocols.

Preparation and characterization

TOPO and CC were weighed into a glass vial at a specific molar ratio. The sealed vial was placed in a 40 kHz ultrasonic water bath and oscillated at 40 °C for 2 hours until the initial solid mixture transformed into a homogeneous, transparent liquid. The product was then left to stand at room temperature for 24 hours. The absence of phase separation or crystallization confirmed the formation of TOPO-CC DES. TOPO-RC DES and TOPO-HQ DES were synthesized using the same method for comparison.

^{31}P NMR spectra were recorded using a Bruker Avance III 600 MHz NMR spectrometer. Absorption spectra in the range of 400–1200 nm were collected using an Agilent Cary 6000i UV-Vis-NIR spectrophotometer.

Solvent extraction

Extraction experiments were conducted in 10 mL stoppered centrifuge tubes. The organic phase consisted of 1.0 mL of the prepared DES. The aqueous phase was 1.0 mL of a nitric acid

This journal is © The Royal Society of Chemistry 2026

Open Access Article. Published on 29 January 2026. Downloaded on 6/15/2026 11:04:01 PM.
This article is licensed under a Creative Commons Attribution-NonCommercial 3.0 Unported Licence.

solution containing a tracer amount of Np(v)-237 (with acidity, salinity, and other conditions adjusted according to experimental design). The two phases were mixed in a thermostatic shaker at 250 rpm for a specified time and then separated by centrifugation at 4000 rpm for 5 minutes. Aliquots of 0.1 mL from each phase were transferred to 10 mL scintillation vials, mixed with 3.0 mL of scintillation cocktail (Hisafe 3), and their radioactivity was measured using a Quantulus 1220 ultra-low background liquid scintillation counter. The distribution ratio (*D*) was defined as $D = C_{\text{org.}}/C_{\text{aq.}}$, where $C_{\text{org.}}$ and $C_{\text{aq.}}$ denote the equilibrium concentrations of the target actinide ion in the organic and aqueous phases, respectively. All extraction experiments were conducted in duplicate to ensure data reliability.

Irradiation test

Irradiation stability assessments were performed utilizing a cobalt-60 (^{60}Co) γ-ray source at Tsinghua University, China. The ^{60}Co source possessed an activity of 1.3×10^{15} Bq, and the absorbed dose rate was adjusted by varying the distance between the sample and the radiation source.

Spectral analysis

A 0.25 mM Np(v) aqueous solution was prepared by diluting a Np(v) stock solution in 1.0 M HNO_3. For spectroscopic measurements, 2.0 mL of the 0.25 mM Np(v) solution in 1.0 M HNO_3 was mixed with an equal volume of either TOPO-CC DES, TOPO-RC DES, or TOPO-HQ DES in a glass vial under continuous stirring to ensure thorough interphase contact. After specified time intervals, the two phases were separated by centrifugation and individually transferred into quartz cuvettes. UV-Vis-NIR spectra were acquired over the wavelength range of 400–1200 nm. TOPO-based DES samples and 1.0 M HNO_3 served as reference solutions for the organic and aqueous phases, respectively. All measurements were carried out at a constant temperature of 298.0 ± 0.1 K, regulated by an external thermostat. Following each spectral measurement, both phases were reintroduced into the original vial, and the procedure of mixing, phase separation, and spectral acquisition was repeated to monitor time-dependent spectral evolution.

Results and discussion

Synthesis and characterization

Based on a molecular functional integration strategy aimed at constructing a novel separation medium with both metal coordination capability and redox activity, we selected TOPO and three dihydroxybenzene isomers (*ortho*-, *meta*-, *para*-) as fundamental building blocks. TOPO serves as a classic neutral phosphine oxide extractant with excellent selectivity and coordination ability for tetravalent actinide ions, yet its coordination with pentavalent neptunyl ($Np^{V}O_2^{+}$) is notably weak,[34,35] which precisely provides the entry point for our functional design. Dihydroxybenzene compounds were chosen as potential reductant-proton synergy components due to their reversible redox couples (dihydroxybenzene/quinone) and proton-donating ability.[36,37] By precisely mixing TOPO (white solid) with CC, RC, or HQ (all solid forms) at a 1 : 1 molar ratio under mild ultrasonication heating conditions (40 °C, 2 hours), we successfully obtained three clear, transparent, and fluid liquids at room temperature: TOPO-CC DES, TOPO-RC DES, and TOPO-HQ DES (Fig. 1). The formation process essentially involves strong intermolecular interactions between the P═O group of TOPO (a strong HBA) and the hydroxyl groups of the dihydroxybenzenes (strong HBDs), forming an extensive hydrogen-bonding network. This network effectively disrupts the crystalline packing of the individual components, significantly depressing the mixture's freezing point below that of any pure component, resulting in a stable liquid phase at room temperature.

Furthermore, we conducted corresponding characterization using nuclear magnetic resonance spectroscopy. The ^{31}P NMR spectra (Fig. 1) show that the characteristic chemical shift of the P atom in pure TOPO is at 48.67 ppm. Upon DES formation, this signal shifts to 52.96 ppm for TOPO-CC DES, 52.29 ppm for TOPO-RC DES, and 51.58 ppm for TOPO-HQ DES. This regular upfield shift is directly attributed to the formation of hydrogen bonds involving the P═O group as the acceptor, which increases the electron shielding around the phosphorus nucleus. The difference in the magnitude of the shift ($\Delta\delta_{\text{CC}} > \Delta\delta_{\text{RC}} > \Delta\delta_{\text{HQ}}$) clearly reflects the isomer-dependent strength of hydrogen bonding. The CC, with its two hydroxyl groups in the *ortho* position, may form a chelating structure *via* intramolecular hydrogen bonding, leading to stronger and more directional intermolecular interactions with the P═O group of TOPO. Additionally, all three newly formed DESs exhibited good fluidity, indicating sufficient mobility for

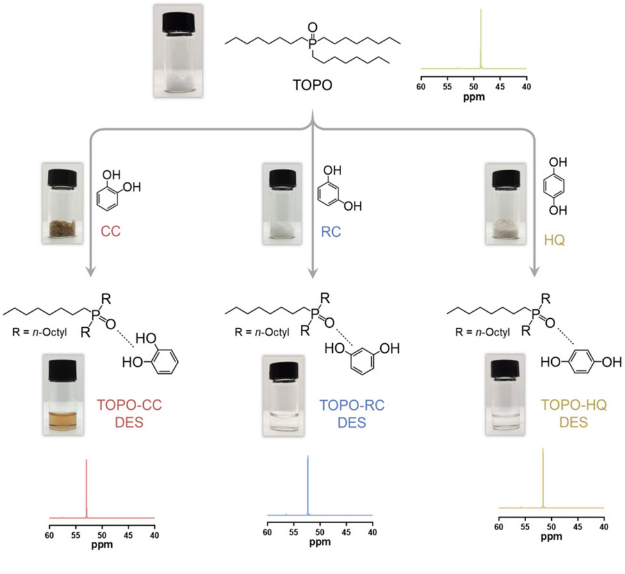

Fig. 1 Structures and graphs of TOPO, CC, RC, HQ, and the corresponding DESs and ^{31}P NMR spectra.

Open Access Article. Published on 29 January 2026. Downloaded on 6/15/2026 11:04:01 PM.
This article is licensed under a Creative Commons Attribution-NonCommercial 3.0 Unported Licence.

mass transfer, and their hydrophobic nature ensured a clear and stable interface for liquid–liquid extraction.

Efficient solvent extraction

Synergistic effects and composition optimization. The core advantage of DESs lies in the tunability of their components and functions. We first systematically investigated the effect of the TOPO to dihydroxybenzene molar ratio (from 1 : 3 to 3 : 1) on the extraction performance of Np(v) (Fig. 2a). For all three DES systems, the distribution ratio D_{Np} showed an almost linear, rapid increase as the TOPO proportion increased from 1 : 3 to 1 : 1. In this initial stage, TOPO, as the key coordination component determining extraction capacity, directly provides more metal-binding sites as its concentration rises. When the molar ratio exceeded 1 : 1, the D_{Np} growth curve entered a plateau, indicating that the coordination sites of TOPO approached saturation at the fixed HBD content, and excess TOPO could not be effectively "activated" to participate in the synergistic process. Therefore, a 1 : 1 molar ratio achieved an economically efficient match between coordination sites and the reducing functional component and was determined as the optimal composition.

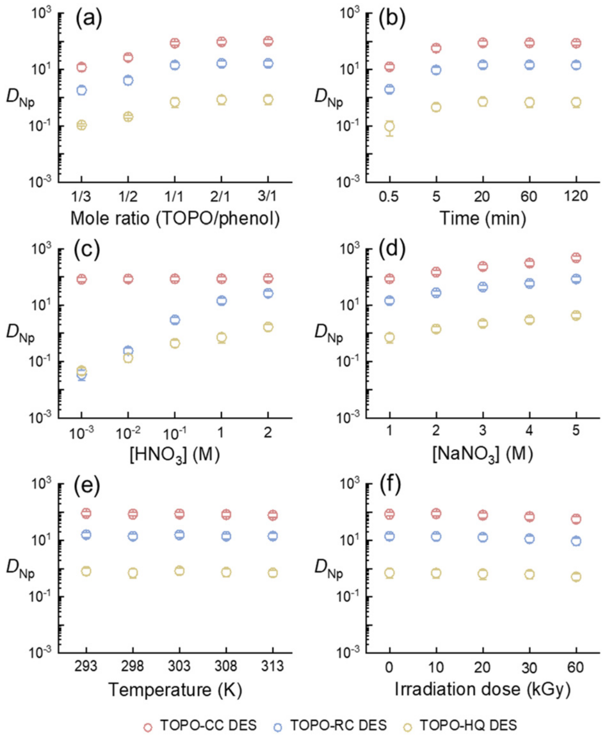

Fig. 2 Effect of (a) DES composition, (b) contact time, (c) HNO_3 concentration, (d) $NaNO_3$ concentration, (e) temperature, and (f) irradiation dose on the extraction of Np(v) by TOPO-dihydroxybenzene DESs. Experimental conditions. Initial organic phase: TOPO-CC DES, TOPO-RC DES, TOPO-HQ DES with mole ratio of (a) 1/3–3/1 and (b–f) 1/1. Initial aqueous phase: trace amount of Np(v)-237 mixed with (a–c, e and f) 1.0 M $NaNO_3$ or (d) 1.0–5.0 M $NaNO_3$ in (a, b and d–f) 1.0 M HNO_3 or (c) 10–3–2.0 M HNO_3 solution. Mixing time: (a and c–f) 120 min, (b) 0.5–120 min. Temperature: (a–d and f) 298.0 ± 0.1 K, (e) 293.0 ± 0.1–313.0 ± 0.1 K.

The stark difference in extraction performance among the three DESs at this optimal ratio (D_{Np}: 85 (TOPO-CC DES) $\gg$ 14 (TOPO-RC DES) > 0.7 (TOPO-HQ DES)) is highly instructive. To exclude the influence of mere solubility or viscosity differences, we performed control experiments. Equimolar amounts of TOPO and dihydroxybenzene were dissolved separately in the traditional inert solvent *n*-dodecane to form molecularly dispersed organic phases, respectively. The results showed that even under these ideally dispersed conditions, the D_{Np} for the TOPO/*n*-dodecane and CC/*n*-dodecane systems were only ~12 and <0.01, respectively, far lower than the 85 achieved by TOPO-CC DES. This strongly demonstrates that the unique, closely-knit hydrogen-bonding network of the DES is not merely a solvent "background" but is crucial for achieving high synergy. We hypothesize that the hydrogen-bonding network may enhance functionality in the following ways. First, it tightly "bundles" TOPO and the dihydroxybenzene at the molecular scale, significantly increasing their local effective concentration in the reaction microenvironment (*e.g.*, the interface). Second, hydrogen bonding may pre-organize the orientation of reactants, lowering the configurational reorganization energy for subsequent electron transfer. Third, it may alter the redox potential of the dihydroxybenzene, making it more prone to releasing electrons.

Kinetics and interfacial process analysis. Extraction kinetics are a key indicator for assessing process feasibility. As shown in Fig. 2b, TOPO-CC DES demonstrated impressively fast extraction capability. At a contact time of only 0.5 min, D_{Np} already exceeded 20, it reached 57 at 5 min (approximately 67% of the equilibrium value), and achieved D_{Np} = 86 at 20 min. Correspondingly, for the TOPO-RC DES system, D_{Np} was 2 at 0.5 min, reached 9 at 5 min, and was 14 at 20 min. For the TOPO-HQ DES system, D_{Np} was 0.1 at 0.5 min, reached 0.46 at 5 min, and was 0.7 at 20 min. All systems reached extraction equilibrium within 20 minutes, indicating good fluid properties and excellent mass transfer kinetics for the DESs. To ensure equilibrium, a contact time of 120 min was used for subsequent experiments.

This rapid kinetics stems from synergistic contributions from multiple aspects. First, the moderate viscosity of the DES ensures adequate molecular diffusion rates. Second, TOPO molecules possess a certain degree of interfacial orientation, favoring the capture of NpO_2^+ from the aqueous phase. Finally, and most importantly, the tight spatial coupling (likely within the same interfacial complex) of the "coordination activation" and "electron transfer" steps avoids long-distance diffusion of reaction intermediates within the phases, dramatically accelerating the overall process.

Tolerance to complex aqueous conditions. Real nuclear waste streams have complex compositions with varying acidity, salinity, and are subject to radiation and temperature fluctuations. Therefore, assessing the robustness of the DES systems under these conditions is crucial.

Acidity is a key factor affecting Np speciation and extraction driving forces. We first examined the effect of HNO_3 concentration on the extraction (Fig. 2c). TOPO-CC DES exhibited an

This journal is © The Royal Society of Chemistry 2026

Open Access Article. Published on 29 January 2026. Downloaded on 6/15/2026 11:04:01 PM. This article is licensed under a Creative Commons Attribution-NonCommercial 3.0 Unported Licence.

almost flat extraction profile (D_{Np} consistently >80) over a wide range from 10^{-3} M to 2.0 M HNO_3. This reveals its unique advantage: the extraction mechanism is not strongly dependent on the aqueous proton concentration. We infer this may be because the reduction process by catechol (CC) involves direct electron transfer or utilizes protons from its own hydroxyl groups, rather than consuming H^+ from the aqueous phase in large quantities. In contrast, the extraction performance of TOPO-RC and TOPO-HQ DES was very poor at low acidity and increased with rising acidity. Specifically, for the TOPO-RC system, D_{Np} increased from 0.03 at 10^{-3} M HNO_3 to 26 at 2 M HNO_3. For the TOPO-HQ system, it increased from 0.04 at 10^{-3} M HNO_3 to 1.6 at 2 M HNO_3. This behavior aligns with a typical proton-coupled electron transfer mechanism, severely limiting their applicability for low-acidity waste streams. The oxidation of diphenols to their corresponding quinones is a two-electron process, with the rate-determining step being the one-electron oxidation that generates the semiquinone radical. The intramolecular hydrogen bond in catechol helps stabilize the radical during oxidation, and as this hydrogen bond locks the proton in place, it partially decouples the deprotonation process from the electron transfer step, resulting in pH-insensitive oxidation kinetics.[38,39] Given the broad acidity universality of TOPO-CC, it is recommended as the optimal system.

Considering the high salinity characteristic of real scenarios, we subsequently analyzed the effect of salt concentration on extraction (Fig. 2d). As the $NaNO_3$ concentration increased from 1 M to 5 M, the D_{Np} for TOPO-CC DES surged from 85 to 470, an increase of over 5-fold. For the TOPO-RC system, D_{Np} increased from 14 at 1 M $NaNO_3$ to 84 at 5 M $NaNO_3$. For the TOPO-HQ system, it increased from 0.26 at 1 M $NaNO_3$ to 0.87 at 5 M $NaNO_3$. These observations indicate that the salting-out effect is also prevalent in DES extraction systems. Quantitative analysis of the salting-out coefficient using the Setschenow equation suggests this effect is significantly stronger than in many traditional extraction systems. High electrolyte concentrations compress the hydration shell of the NpO_2^+ ion, reducing its hydration energy and enhancing its lipophilicity, making it more prone to transfer into the organic phase.[40] This property holds great potential for treating high-salinity simulated waste streams and similar scenarios.

In view of the potential for radiolytic heating, we then examined the effect of temperature on extraction (Fig. 2e). Over the typical ambient temperature range of 293 K to 313 K, the distribution ratios changed only minimally. Specifically, for the TOPO-CC system, D_{Np} decreased from 90 at 293 K to 77 at 313 K. For the TOPO-RC system, D_{Np} changed from 16 to 14 over the same range, and for the TOPO-HQ system, it decreased from 0.81 to 0.69. This insensitivity to temperature changes is essentially related to the extraction thermodynamics of TOPO.[41–43] It suggests the extraction process is entropy-driven, with the primary driving force likely stemming from the release of ordered water molecules surrounding the metal ion upon formation and transfer of the Np(IV) complex into the organic phase, leading to an increase in system entropy. This weak temperature dependence simplifies process control requirements.

Given the strong radiation fields in real scenarios, we further investigated the effect of different gamma irradiation doses on extraction (Fig. 2f). At cumulative absorbed doses of 0 and 10 kGy, the D_{Np} values for TOPO-CC DES, TOPO-RC DES, and TOPO-HQ DES were 85, 14.1, 0.71 and 88, 13.7, 0.69, respectively, showing almost no significant change. Even at a high dose of 60 kGy, the D_{Np} for TOPO-CC DES decreased from 85 to 57, still maintaining considerable activity, far exceeding the performance of most reported systems.[44–50]

These above-results demonstrate that the constructed DESs, especially TOPO-CC, enable the *in situ* reduction and highly efficient extraction of Np(V) without introducing additional reagents. Moreover, they exhibit excellent kinetic properties and broad applicability under wide ranges of acidity, high salinity, temperature, and high irradiation doses, highlighting their stability, anti-interference capability, and suitability for various process/environmental scenarios.

Mechanistic insights

Spectral analysis. To visually reveal the fate of Np(V) during the extraction process, we performed *in situ*, real-time monitoring of both phases using UV-Vis-NIR spectroscopy (Fig. 3a). The characteristic fingerprint peak of Np(V) in the initial aqueous phase at 980 nm (attributed to the f–f electronic transition of NpO_2^+, $\varepsilon \approx 395$ M^{-1} cm^{-1}) served as the monitoring indicator. Upon contact with TOPO-CC DES, the intensity of this aqueous peak plummeted by over 93% within 10 seconds (Fig. 3c), while simultaneously, distinct characteristic peaks of Np(IV) appeared in the organic phase at 723 nm ($\varepsilon \approx 190$ M^{-1} cm^{-1}) and 960 nm ($\varepsilon \approx 175$ M^{-1} cm^{-1}) (Fig. 3b). Quantitative analysis showed that the conversion rate from Np(V) to Np(IV) exceeded 98% within 5 minutes, and the Np(V) signal in the aqueous phase nearly disappeared after 120 minutes. This spectral evolution provides direct and powerful evidence for "*in situ* reduction."

Comparative experiments clearly demonstrated the decisive influence of HBD structure on reduction kinetics and efficiency (Fig. 3d–g). For the TOPO-RC DES system, the reduction percentages of Np(V) at contact times of 10 seconds, 5 minutes, and 120 minutes were approximately 50%, 85%, and 90%, respectively. The corresponding percentages for the TOPO-HQ DES system were lower, at 30%, 49%, and 76%, respectively. This significant difference in reducing capability (CC ≫ RC > HQ) aligns perfectly with the order of extraction performance (TOPO-CC DES ≫ TOPO-RC DES > TOPO-HQ DES), directly attributing the root cause of performance disparity to the electron-donating ability of the dihydroxybenzene isomers. The CC with its two hydroxyl groups in the *ortho* position, is more readily oxidized to form stable *o*-benzoquinone, resulting in greater thermodynamic driving force and superior kinetics.

Identification of coordination sites. Given the extreme difficulty of direct structural analysis of highly radioactive Np complexes, we employed U(VI) (UO_2^{2+}), which possesses a

Open Access Article. Published on 29 January 2026. Downloaded on 6/15/2026 11:04:01 PM.
This article is licensed under a Creative Commons Attribution-NonCommercial 3.0 Unported Licence.

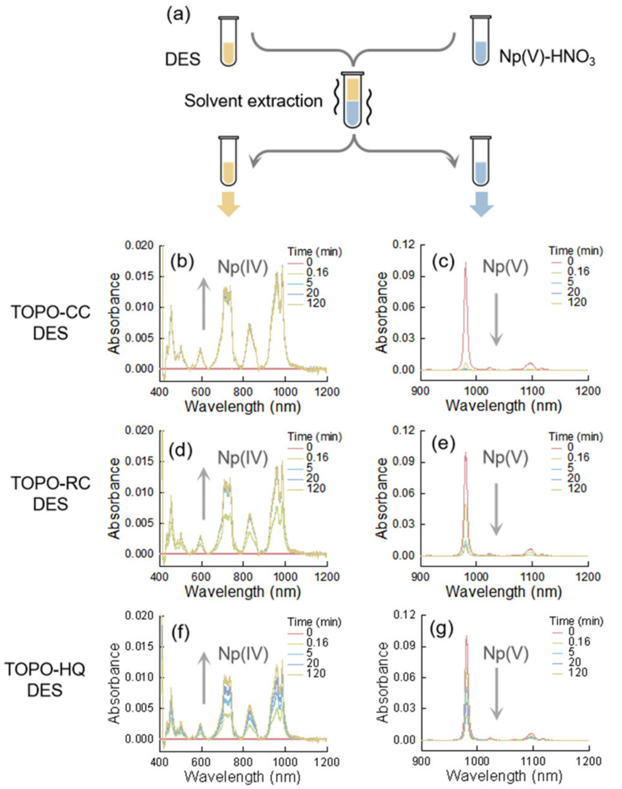

Fig. 3 (a) Schematic diagram of the solvent extraction and spectroscopic monitoring of Np(v) using TOPO-dihydroxybenzene DESs. Variation of the absorption spectra in the (b, d and f) organic phase and the (c, e and g) aqueous phase after mixing TOPO-dihydroxybenzene DESs with Np(v)/HNO_3 solution. Experimental conditions. Initial organic phase: (b and c) TOPO-CC DES (1/1), (d and e) TOPO-RC DES (1/1), (f and g) TOPO-HQ DES (1/1). Initial aqueous phase: 0.25 mM Np(v) in 1.0 M HNO_3. Mixing time: 0–120 min. Temperature: 298.0 ± 0.1 K.

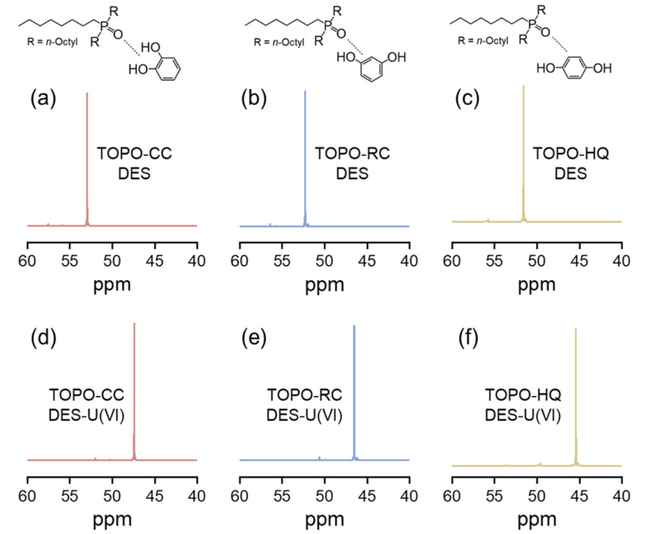

Fig. 4 Comparison of "free" and U(vi)-incorporated TOPO-dihydroxybenzene DESs through ^{31}P NMR spectra. (a) TOPO-CC DES, (b) TOPO-RC DES, (c) TOPO-HQ DES, (d) TOPO-CC DES-U(vi), (e) TOPO-RC DES-U(vi), (f) TOPO-HQ DES-U(vi).

similar linear dioxo structure (Actinyl, AnO_2^{n+}), as a low-radioactivity model ion to investigate the coordination mode of the DESs using ^{31}P NMR (Fig. 4). Upon loading with U(vi), the ^{31}P signals of TOPO in all DESs underwent significant upfield shifts. The shift values ($\Delta\delta$) were: TOPO-CC DES-U (5.54 ppm), TOPO-RC DES-U (5.78 ppm), and TOPO-HQ DES-U (6.16 ppm). This change unambiguously confirms that the P═O group of TOPO serves as the primary coordination site for the metal ion. It is noteworthy that the order of the absolute shift values does not show a simple linear correlation with the order of hydrogen bond strength, reducing capability, or extraction efficiency. This may be due to differences in the coordination mode of U(vi) compared to Np(v/iv), or complex modulation of the coordination microenvironment by the presence of the dihydroxybenzene. Nevertheless, the core conclusion of this experiment is definitive: within the DES, TOPO retains its essential coordinating function as a neutral phosphine oxide extractant.

Elucidation of the synergistic mechanism. Integrating all the experimental evidence, we propose and elaborate a panoramic view of the "coordination-driven reduction" synergistic mechanism for Np(v) extraction by the TOPO-dihydroxybenzene DES systems (Fig. 5). This mechanism consists of four closely linked steps.

(1) Interfacial enrichment and pre-coordination. Due to their amphiphilic nature, TOPO molecules tend to orient at the oil–water interface, with hydrophobic alkyl chains extending into the organic phase and polar P═O groups pointing towards the aqueous phase. Although the coordination constant between $Np^VO_2^+$ and a single P═O group is small, under the high local concentration of TOPO at the interface, a dynamic, weakly bound "outer-sphere" or "ion-pair" type intermediate, $[NpO_2^+\cdots(TOPO)_n]$ interface, can form rapidly. This step selectively enriches Np(v) from the bulk aqueous solution into the confined reaction zone at the interface.

(2) Coordination activation and potential modulation. This step is the core and innovative aspect of the mechanism. The σ-donor interaction from the P═O group of TOPO to the Np

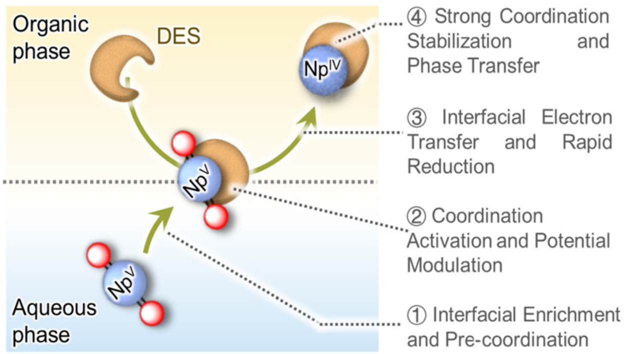

④ Strong Coordination Stabilization and Phase Transfer
③ Interfacial Electron Transfer and Rapid Reduction
② Coordination Activation and Potential Modulation
① Interfacial Enrichment and Pre-coordination

Fig. 5 Schematic illustration of the *in situ* complexation, reduction, and extraction of Np by the TOPO-dihydroxybenzene DESs system.

Open Access Article. Published on 29 January 2026. Downloaded on 6/15/2026 11:04:01 PM.
This article is licensed under a Creative Commons Attribution-NonCommercial 3.0 Unported Licence.

center increases the electron density on Np, particularly feeding back into the antibonding 5f orbitals. This effectively lowers the energy required for the reduction from Np(v) (f^2) to Np(IV) (f^3), *i.e.*, significantly reduces the formal redox potential (E) of the Np(v)/Np(IV) couple. This "coordination activation" effect transforms the originally thermodynamically unfavorable reduction reaction ($E_{\mathrm{Np(V)/Np(IV)}}$ is approximately +1.0 V *vs.* SHE in 1 M HNO_3) into one that falls within the reducing capability of the dihydroxybenzene.

(3) Interfacial electron transfer and rapid reduction. The activated interfacial Np(v)-TOPO intermediate becomes an ideal acceptor for the interfacial electron transfer reaction. Dihydroxybenzene molecules (especially CC with the most negative reduction potential) dissolved in the organic phase near the interface act as electron donors. Through direct contact or quantum tunneling at the interface, they efficiently transfer electrons to the Np(v) center. This step may be accompanied by proton transfer to stabilize the product, with protons potentially coming from the dihydroxybenzene itself or the aqueous phase. The rapid electron transfer ensures the reduction step does not become rate-limiting for the overall process.

(4) Strong coordination stabilization and phase transfer. The generated Np(IV) ion has distinctly different coordination chemistry compared to Np(v). It exhibits extremely high affinity for TOPO and can rapidly combine with 2 TOPO molecules and 4 nitrate ions (from either the aqueous phase or the DES microenvironment) to form a neutral, highly hydrophobic complex, $Np(NO_3)_4{\cdot}2TOPO$.[51] This complex desorbs from the interface and fully dissolves into the bulk hydrophobic DES phase. At this point, the Np atom completes its full transformation from aqueous $Np^{V}O_2^{+}$ to organic Np(IV)-TOPO complex, achieving the perfect unification of reduction and extraction in both time and space.

The elegance of this mechanism lies in its molecular design, which integrates the two originally separate functional modules, "coordination" (TOPO) and "reduction" (dihydroxybenzene), at the nanoscale *via* the DES hydrogen-bonding network. Their synergistic action at the special reaction field of the liquid–liquid interface efficiently addresses the challenge of capturing Np(v).

Conclusions

This study successfully designed and constructed a novel series of functionalized hydrophobic DESs based on TOPO and dihydroxybenzene isomers. It provides, for the first time, a comprehensive demonstration of their exceptional capability for efficient, rapid, *in situ* reduction and integrated extraction of Np(v) from nitric acid media. Notably, the TOPO-CC DES system exhibited outstanding performance, maintaining excellent extraction efficiency (D_{Np} up to 470) and fast mass transfer/reduction kinetics (Np(v) reduction ratio >98% within 5 minutes) under simulated harsh conditions including wide acidity (10^{-3} to 2.0 M HNO_3), high salinity (1.0–5.0 M $NaNO_3$), broad temperature range (293–313 K), and strong gamma irradiation (cumulative dose up to 60 kGy). Through multifaceted mechanistic investigations, including *in situ* spectroscopic monitoring and coordination chemistry studies, we revealed and confirmed the unique "coordination-driven reduction" synergistic mechanism. TOPO not only acts as the final extractant but, more critically, activates Np(v) *via* interfacial pre-coordination, significantly lowering its reduction barrier. The dihydroxybenzene component acts as an efficient built-in electron donor. Particularly, catechol (*ortho*-dihydroxybenzene), with its two hydroxyl groups in *ortho*-position, exhibits stronger electron-donating ability compared to its *meta*- and *para*-isomers. This enhances the stability of reaction intermediates and reduces the energy barrier. Such a structure facilitates rapid electron transfer at the interface, generating Np(IV) that is readily captured by strong TOPO coordination, ultimately achieving the integrated coupling of the "coordination–activation–reduction–extraction" process. This work not only offers a green, robust, and promising new technological strategy for addressing the longstanding challenge of Np(v) separation in nuclear fuel cycles but also, by creating and deeply understanding this "coordination–reduction" dual-functional integrated solvent system, provides a new paradigm for the design and mechanistic study of novel functional materials tailored for complex separation needs, holding significant scientific importance and application foresight.

Author contributions

L. Z., and Q. L. T., conceived the experiments, supervised the studies, collected and analyzed the data. Z. P. W wrote the manuscript. C. X., and Z. P. W. participated in the discussion.

Conflicts of interest

There are no conflicts to declare.

Data availability

Data will be made available on request.

Acknowledgements

C. Xu acknowledges the financial support from National Natural Science Foundation of China (22325603, U2541251). Z. P. Wang acknowledges the financial support from National Natural Science Foundation of China (22376116) and Youth Talent Project of China National Nuclear Corporation.

Open Access Article. Published on 29 January 2026. Downloaded on 6/15/2026 11:04:01 PM.
This article is licensed under a Creative Commons Attribution-NonCommercial 3.0 Unported Licence.

References

1 R. Wigeland, T. H. Bauer, T. Fanning and E. Morris, Separations and transmutation criteria to improve utilization of a geologic repository, *Nucl. Technol.*, 2006, **154**, 95–106.

2 H. Cao, Y. Guo, B. Li, Q. Tang, H. Hao, Z. Wang and C. Xu, Extraction and complexation of trivalent americium and lanthanides using an asymmetric picolinic acid-derived tridentate N,O-hybrid ligand, *Dalton Trans.*, 2025, **54**, 1964–1971.

3 Z. Wang, H. Huang, S. Ding, X. Hu, L. Zhang, Y. Liu, L. Song, Z. Chen and S. Li, Extraction of trivalent americium and europium with TODGA homologs from HNO_3 solution, *J. Radioanal. Nucl. Chem.*, 2017, **313**, 309–318.

4 Z. Wang, F. Li, X. Wang, B. Li, L. Song, X. Yang, Q. Xiao, H. Tang and S. Ding, Demonstration of a continuous counter-current extraction process based on a non-heterocyclic N-donor ligand NTAamide(*n*-Oct) for trivalent actinides/lanthanides separation, *Sep. Purif. Technol.*, 2021, **261**, 118285.

5 H. Hao, Y. Liu, H. Cao, Z. Wang, C. Xu and J. Chen, An insightful study on the reduction and extraction of neptunium assisted by molybdenum, *Dalton Trans.*, 2024, **53**, 17909–17917.

6 S. Chatterjee, S. A. Bryan, A. J. Casella, J. M. Peterson and T. G. Levitskaia, Mechanisms of neptunium redox reactions in nitric acid solutions, *Inorg. Chem. Front.*, 2017, **4**, 581–594.

7 H. Hao, Y. Liu, X. Dong, Y. Guo, B. Li, S. Liu, C. Xu, J. Chen and Z. Wang, A straightforward organic complexation strategy enables precise and efficient oxidation state control of Np, *Sci. China: Chem.*, 2025, **68**, 3071–3077.

8 H. Hao, S. Zhang, X. Dong, Q. Tang, Y. Guo, Y. Liu, J. Chen, J. Su, Z. Wang and C. Xu, Coordination-driven in-situ reduction and extraction of neptunium, *Sci. China: Chem.*, 2025, DOI: 10.1007/s11426-025-2866-x.

9 G. R. Choppin and l. F. Rao, Complexation of pentavalent and hexavalent actinides by fluoride, *Radiochim. Acta*, 1984, **37**, 143–146.

10 G. R. Choppin, Solution Chemistry of the actinides, *Radiochim. Acta*, 1983, **32**, 43–54.

11 B. Acevedo, K. V. Hecke, T. Cardinaels and M. Verwerft, ^{238}Pu production: a state-of-the-art review of NpO_2 target fabrication technologies and processing of irradiated targets, *Radiochim. Acta*, 2023, **111**, 857–885.

12 H. Hao, Y. Guo, B. Li, Q. Tang, Y. Liu, X. Dong, C. Xu, J. Chen and Z. Wang, Mechanistic insights into molybdenum-iron-catalyzed neptunium reduction and extraction, *Inorg. Chem.*, 2025, **64**, 10542–10548.

13 X. Yang, Y. Wang, D. Fang, X. Xu, A. Zhang and C. Xiao, Selective Np(V) extraction by unsymmetrical amide-triazine-pyridine ligand enabling simplified actinide separation, *Dalton Trans.*, 2026, DOI: 10.1039/D5DT02851E.

14 X. Yang, Y. Wang, D. Fang, S. Wang, Z. Li, A. Zhang and C. Xiao, Efficient Coextraction of U(VI), Np(V), and Pu(IV) Using Tetradentate N-Heterocyclic Amide-Triazine Extractants, *Chem Bio Eng.*, 2025, DOI: 10.1021/cbe.5c00086.

15 C.-L. Xiao, Q.-Y. Wu, C.-Z. Wang, Y.-L. Zhao, Z.-F. Chai and W.-Q. Shi, Quantum Chemistry Study of Uranium(VI), Neptunium(V), and Plutonium(IV,VI) Complexes with Preorganized Tetradentate Phenanthrolineamide Ligands, *Inorg. Chem.*, 2014, **53**, 10846–10853.

16 X. Huang, X.-B. Li, Q.-Y. Wu and W.-Q. Shi, Experimental and theoretical progress on the reduction of Np(vi) with salt-free reagents in the PUREX process, *Ind. Chem. Mater.*, 2025, **3**, 412–430.

17 X. Huang, X. Li, Q. Wu, C. Wang, J. Lan, H. Wang and W. Shi, Uncovering the reduction mechanism of Np(vi) with N,N-diethyl hydroxylamine: a scalar-relativistic DFT investigation, *Phys. Chem. Chem. Phys.*, 2024, **26**, 27395–27405.

18 X. Yang, L. Xu, A. Zhang and C. Xiao, Organophosphorus extractants: a critical choice for actinides/lanthanides separation in nuclear fuel cycle, *Chem. – Eur. J.*, 2023, **29**, e202300456.

19 V. P. Shilov and A. M. Fedoseev, Mechanism of transformation of Np(V) into Np(IV) in sodium 1,2-cyclohexanediaminetetraacetate solutions, *Sov. Radiochem.*, 2016, **58**, 586–590.

20 T. Nakamura, M. Takahashi, T. Fukasawa and M. Utamura, Kinetics of reduction of Np(V) to Np(IV) by platinum black as reduction catalyst, *J. Nucl. Sci. Technol.*, 1992, **29**, 393–395.

21 V. S. Koltunov, S. M. Baranov and G. V. Koltunov, Kinetics of reactions of Np and Pu ions with hydrazine derivatives: XVIII. reaction between Np(V) and hydroxyethylhydrazine, *Sov. Radiochem.*, 2005, **47**, 168–172.

22 A. Ikeda-Ohno, C. Hennig, A. Rossberg, H. Funke, A. C. Scheinost, G. Bernhard and T. Yaita, Electrochemical and Complexation Behavior of Neptunium in Aqueous Perchlorate and Nitrate Solutions, *Inorg. Chem.*, 2008, **47**, 8294–8305.

23 Y. Kitatsuji, T. Kimura and S. Kihara, Reduction behavior of neptunium(V) at a gold or platinum electrode during controlled potential electrolysis and procedures for electrochemical preparations of neptunium(IV) and (III), *J. Electroanal. Chem.*, 2010, **641**, 83–89.

24 G. F. Kessinger, E. A. Kyser and P. M. Almond, Literature review: reduction of Np(V) to Np(IV)-alternatives to ferrous sulfamate, Advanced Fuel Cycle Initiative, SRNL-STI-2009–00610, Savannah River National Laboratory: Aiken, SC, 2009, DOI: 10.2172/969037.

25 G. Zante and M. Boltoeva, Review on hydrometallurgical recovery of metals with deep eutectic solvents, *ACS Sustainable Chem. Eng.*, 2020, **1**, 238–255.

26 Z. Yuan, H. Liu, W. F. Yong, Q. She and J. Esteban, Status and advances of deep eutectic solvents for metal separation and recovery, *Green Chem.*, 2022, **24**, 1895–1929.

27 Y. Yu, Q. Tang, J. Chen and Z. Wang, Oxidative eutectic mixture for efficient decontamination of environmental radioactivity, *Water Res.*, 2026, **291**, 125162.

This journal is © The Royal Society of Chemistry 2026

Open Access Article. Published on 29 January 2026. Downloaded on 6/15/2026 11:04:01 PM.
This article is licensed under a Creative Commons Attribution-NonCommercial 3.0 Unported Licence.

28 M. Gilmore, É.N McCourt, F. Connolly, P. Nockemann, M. Swadźba-Kwaśny and J. D. Holbrey, Hydrophobic deep eutectic solvents incorporating trioctylphosphine oxide: advanced, liquid extractants, *ACS Sustainable Chem. Eng.*, 2018, **6**, 17323–17332.

29 D. J. G. P. van Osch, D. Parmentier, C. H. J. T. Dietz, A. van den Bruinhorst, R. Tuinier and M. C. Kroon, Removal of alkali and transition metal ions from water with hydrophobic deep eutectic solvents, *Chem. Commun.*, 2016, **52**, 11987–11990.

30 H. Hao, Q. Tang, C. Zhao, Y. Liu, C. Xu, J. Chen and Z. Wang, Redox-functionalized eutectic mixtures enable efficient actinide group recovery, *ACS Sustainable Resour. Manage.*, 2025, **2**, 2327–2336.

31 Q. Tang, H. Hao, C. Xu, S. Liu and Z. Wang, Synergistic coordination-encapsulation in eutectic mixture enables robust lanthanides capture at multi-scenarios, *Sep. Purif. Technol.*, 2026, **382**, 136000.

32 D. O. Abranches and J. A. P. Coutinho, Everything YouWanted to Know about Deep Eutectic Solvents butWere Afraid to Be Told, *Annu. Rev. Chem. Biomol. Eng.*, 2023, **14**, 141–163.

33 S. Banerjee, P. K. Mohapatra, A. Bhattacharyya, S. Basu and V. K. Manchanda, Extraction of tetravalent neptunium isoxazolonates as their TOPO adducts, *Radiochim. Acta*, 2004, **92**, 95–100.

34 R. Shabana and H. Ruf, Extraction and Separation of neptunium, uranium, thorium and cerium with TOPO from mixed solvents, *Radiochim. Acta*, 1976, **23**, 117–120.

35 Y. Inoue and O. Tochiyama, Solvent extraction of neptunium(V) by thenoyltrifluoroacetone and 1,10-phenanthroline or tri-n-octylphosphine oxide, *Radiochim. Acta*, 1982, **31**, 193–196.

36 J. W. Herbert and D. H. Macartney, Kinetics of the reduction of a tetra-μ-acetato-dirhodium cation by substituted 1,2- and 1,4-dihydroxybenzene compounds in aqueous perchlorate media, *J. Chem. Soc.*, 1986, **9**, 1931–1935.

37 N. S. Shcherbina, I. V. Perminova, S. N. Kalmykov, A. N. Kovalenko, R. G. Haire and A. P. Novikov, Redox and complexation interactions of neptunium(V) with quinonoid-enriched humic derivatives, *Environ. Sci. Technol.*, 2007, **41**, 7010–7015.

38 T. Shanmugaprabha, K. Selvakumar, M. Vairalakshmi, K. Rajasekaran and P. Sami, Proton-coupled electron transfer reactions: kinetic studies on the oxidation of dihydroxybenzenes by heteropoly 10-tungstodivanadophosphate in aqueous acidic medium, *Transition Met. Chem.*, 2015, **40**, 197–205.

39 V. Lukeš, A. Kováčová and H. Hartmann, On thermodynamics of electron, proton and PCET processes of catechol, hydroquinone and resorcinol – Consequences for redox properties of polyphenolic compounds, *J. Mol. Liq.*, 2022, **360**, 119356.

40 B. Naseem, I. Arif and M. A. Jamal, Kosmotropic and chaotropic behavior of hydrated ions in aqueous solutions in terms of expansibility and compressibility parameters, *Arabian J. Chem.*, 2021, **14**, 103405.

41 G. Suresh, M. S. Murali and J. N. Mathur, Thermodynamics of extraction of Am(III) and Eu(III) from different anionic media with Tri-n-octyl phosphine oxide, *Radiochim. Acta*, 2003, **91**, 127–134.

42 M. R. Yaftian, M. E. Eshraghi and L. Hassanzadeh, Extractive properties of tri-*n*-octylphosphine oxide towards thorium(IV) and europium(III) ions in aqueous nitrate media, *Iran. J. Chem. Eng.*, 2003, **22**, 71–76.

43 U. G. Favero, N. Schaeffer, H. Passos, K. A. M. L. Cruz, D. Ananias, S. Dourdain and M. C. Hespanhol, Solvent extraction in non-ideal eutectic solvents – application towards lanthanide separation, *Sep. Purif. Technol.*, 2023, **314**, 123592.

44 J. I. Bullock and D. G. Tuck, The solvent extraction of neptunium(V) and (VI) species: limitations in the use of amine extraction in the study of complex formation, *J. Inorg. Nucl. Chem.*, 1971, **33**, 3891–3904.

45 I. Svantesson, G. Persson, I. Hagström and J. O. Liljenzin, Distribution ratios and empirical equations for the extraction of elements in Purex high level waste solution—II: HDEHP, *J. Inorg. Nucl. Chem.*, 1980, **42**, 1037–1043.

46 D. Wisnubroto, S. Nagasaki, Y. Enokida and A. Suzuki, Effect of tbp on solvent extraction of Np(V) with m-octyl (phenyl)-, *N*,*N* diisobutylcarbamoylmethylphosphine oxide, *J. Nucl. Sci. Technol.*, 1992, **29**, 263–268.

47 Y. Sasaki and G. R. Choppin, Extraction of Np(V) by *N*,*N*'-dimethyl-*N*,*N*'-dihexyl-3-oxapentanediamide, *Radiochim. Acta*, 1998, **80**, 85–88.

48 W. Jianchen and S. Chongli, Hot test of trialkyl phosphine oxide (TRPO) for removing actinides from highly saline high-level liquid waste (HLLW), *Solvent Extr. Ion Exch.*, 2001, **19**, 231–242.

49 Y. Sasaki, Y. Tsubata, Y. Kitatsuji, Y. Sugo, N. Shirasu, Y. Morita and T. Kimura, Extraction behavior of metal ions by TODGA, DOODA, MIDOA, and NTAamide extractants from HNO_3 to n-dodecane, *Solvent Extr. Ion Exch.*, 2013, **31**, 401–415.

50 J. M. Gogolski, P. R. Zalupski, T. S. Grimes and M. P. Jensen, Neptunium extraction by *N*,*N*-dialkylamides, *Radiochim. Acta*, 2020, **108**, 707–716.

51 S. Banerjee, P. K. Mohapatra, A. Bhattacharyya, S. Basu and V. K. Manchanda, Extraction of neptunium(IV) by a mixture of 3-phenyl-4-acetyl-5-isoxazolone and tri-n-octyl phosphine oxide, *Radiochim. Acta*, 2006, **94**, 313–317.